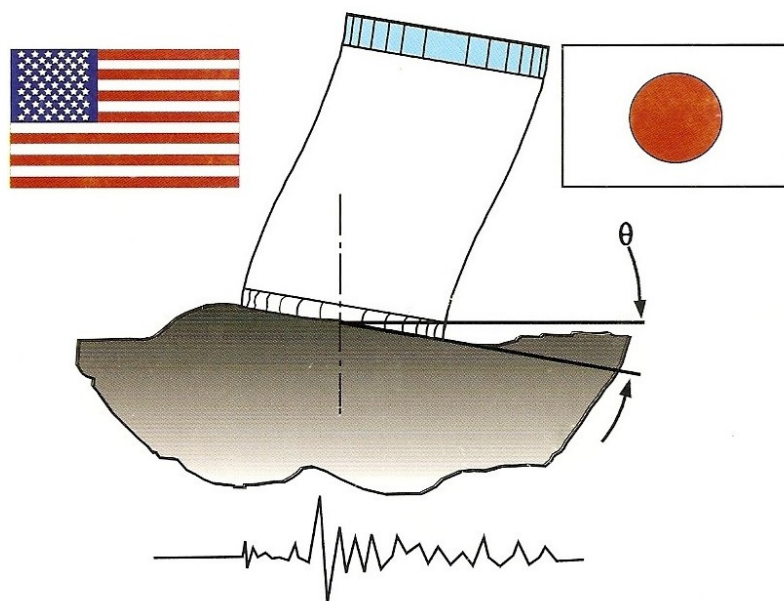


**Proceedings**  
**UJNR WORKSHOP ON**  
**SOIL-STRUCTURE INTERACTION**

**Menlo Park, California**  
**September 22-23, 1998**



**Editors & Conveners:**

**Mehmet Celebi<sup>1</sup>**  
**and**  
**Izuru Okawa<sup>2</sup>**

**Open-File Report 99-142**  
**1999**

*This report is preliminary and has not been reviewed for conformity with U.S. Geological Survey editorial standards (or with the North American Stratigraphic Code). Any use of trade, product or firm names is for descriptive purposes only and does not imply endorsement by the U.S. Government.*

**U.S. Department of the Interior**  
**U.S. Geological Survey**

<sup>1</sup> U.S. Geological Survey (MS977), 345 Middlefield Rd., Menlo Park, Ca. 94025

<sup>2</sup> IISEE, Building Research Institute, Tsukuba, Japan

# Uncertainties of Seismic Soil-Structure Interaction Analysis: Significance, Modeling and Examples

D. M. Ghiocel, Ph.D.

*STI Technologies, Inc., Rochester, NY 14623*

**ABSTRACT:** The aim of this paper is to (i) discuss the significance of different uncertainty sources on seismic soil-structure interaction (SSI), (ii) review the engineering current practice for assessing SSI uncertainty effects using probabilistic models and finally (iii) propose a new procedure for an accurate probabilistic SSI analysis. The intention of the paper is not to address all significant SSI aspects, but only few of these which based on author's opinion are not consistently reflected by the current state-of-engineering practice. Several shortcomings of the current engineering practice for assessing structural risks for critical facilities are pointed out. The proposed procedure uses for the idealization of seismic input and soil properties stochastic field models. Its implementation offers a significant advancement for performing probabilistic seismic SSI analyses.

## INTRODUCTION

The factors influencing SSI are a myriad. This is due to the complexity of seismic SSI phenomenon. A short list of major factors influencing SSI may include:

### Wave propagation:

- control motion, including intensity, directionality, frequency content
- wave composition, including internal waves, P and S, with surface waves, Rayleigh and Love, and other wave types
- spatial variation of ground motion with depth and distance, including motion
- incoherency and wave passage effects
- soil nonlinear behavior as a function of shear strain in soil, soil stability

### Soil-structure interaction:

- wave scattering effects or kinematic interaction
- dynamic characteristics of structure-foundation-soil ensemble, including

- embedment effects on system stiffness and vibration energy radiation
- structure nonlinear behavior, which may be more ductile or brittle, including
- stiffness degradations and damping increase
- local contact interface nonlinearities between soil and foundation

SSI response depends drastically on both the seismic environment and structure-foundation-soil ensemble dynamic characteristics.

The seismic SSI uncertainties are usually divided in two major source types of uncertainties, namely: (i) uncertainties due to inherent randomness in natural phenomena induced by earthquakes and in material properties, and (ii) uncertainties due to modeling uncertainties in SSI models and assumptions.

To illustrate the contributions of the two types of uncertainty sources, the probabilistic seismic response of a nuclear power plant (NPP) is considered (Ghiocel et al., 1994). Figure 1 shows the simulated in-structure spectra for the Reactor Building (RB), at the basemat and the top of the

containment, and for the Auxiliary Building (AB), at the roof level. The SSI effects are larger for the RB than for AB. The random variability in the spectral response is higher at the top elevations than for the basemat. This indicates that the SSI uncertainties are mostly propagated through the rocking motion than through the horizontal motion. The contributions of two types of uncertainty on seismic response of the two NPP buildings are quantified in Figure 2. The two spectral curves correspond to coefficient of variation curves which were computed assuming that the uncertainties are

There are two major avenues for improving SSI modeling uncertainties: (i) improve deterministic SSI prediction models and (ii) improve probabilistic models. These two avenues are discussed in the next two sections.

#### DETERMINISTIC PREDICTION MODELS

There are many significant SSI aspects with significant impact on accuracy of seismic structural predictions which are not appropriately considered by the present state-of-engineering practice. Herein, only few of these aspects, subjectively selected, are addressed.

Table 1. Structural Fragility Analysis Results for the investigated NPP

Building	$\beta_R$	$\beta_U$	$\beta_C$	Median Capacity	HCLPF Capacity
Reactor Building (Basemat Failure)	0.43	0.32	0.54	2.31g	0.70g
Auxiliary Building (Steel Columns)	0.33	0.29	0.44	2.50g	0.90g
Penetration Area (Concrete Wall)	0.32	0.27	0.42	1.19g	0.45g
Intake Structure	0.31	0.26	0.40	1.40g	0.55g
Diesel Gen. Building (Concrete Slab)	0.32	0.25	0.41	1.24g	0.49g

due to inherent randomness in the input motion frequency content and soil properties, and that the uncertainties are due to both the inherent randomness and the modeling uncertainties, respectively. The final results of the seismic probabilistic risk assessment (SPRA) calculations for the investigated NPP are shown in Table 1. The results indicate that the two uncertainty sources, i.e. randomness and modeling, contribute almost equally to the total seismic response uncertainty. They are typical for NPPs founded on soil sites and consistent with the present state-of-the-engineering knowledge and practice. The paper focus is limited to SSI modeling uncertainties.

One major aspect which is a significant barrier against SSI modeling accuracy is the limitation of currently available computational tools for performing efficiently rigorous nonlinear SSI analyses, including both wave propagation aspects and soil/structure nonlinear behavior aspects. Using the most currently applied computer programs such as SASSI, CLASSI, DRAIN, ADINA, ANSYS, ABAQUS, etc. there are strong limitations for rigorous nonlinear SSI analyses. The limitations are due to the computational effort, program capability and professional qualification and effort associated with the use of different computer programs. As a consequence of this situation, the SSI practical procedures include significant conservatism to cover the simplified assumptions made. On the

other side, simplified investigations may generate an uneconomical design due to higher stresses in structures. One may think more seriously to the potential savings coming from applying a more refined SSI analysis while designing or retrofitting a concrete highway bridge within the US. Any simplified conservative assumption on modeling of SSI effects, including structural/soil nonlinear behavior and local wave propagation/scattering effects, may induce additional cost of millions of dollars.

Other significant SSI aspects which need more attention and more adequate consideration in the future engineering practice are related to the evaluation of (i) torsional effects induced in structures with mass eccentricities and large size foundations due to motion incoherency, including wave passage effects, and structure-soil-structure interaction effects between neighboring structures, especially for massive, deeply embedded or buried structures. An important modeling SSI uncertainty is related to the computation of seismic pressures on embedded walls and deep foundations. Other aspect which in practice sometime is of a great interest is the local soil instability effects, especially liquefaction, on SSI response. To highlight the SSI aspects selected case study results are briefly discussed as shown Figures 3 through 10.

Figure 3 shows the in-structure spectra computed in an axisymmetric model of a Reactor Building founded on a soft soil, i.e. shear wave velocity of 1000 fps, at the basemat at the edge due to torsional accelerations and at the top of internal structure due to horizontal translational accelerations. The motion incoherency was idealized using a Luco-Wong model (Luco and Wong, 1986) with a coherence parameter of 0.30, which corresponds to an upperbound of incoherency. For this value, the computed peak acceleration due to torsional motion is 30% of the peak acceleration due to horizontal translation. The SSI calculations were done with the ACS SASSI/PC computer program (Ghiocel, 1997). This computer program is based on the original SASSI program, but has significant additional capabilities, including motion incoherency and multiple excitation options. Torsional motions induced by incoherency can have a severe effect on

nonsymmetric structures with large mass eccentricities.

Figure 4 shows the seismic pressure computed on the lateral wall of a typical, flexible buried waste storage tank (WST) filled with liquid, using a Beredugo-Novak lumped parameter SSI model (Miller and Costantino, 1994) and a SASSI model. The computed pressure distribution has different shapes for the two SSI models. Further, Figure 5 shows the effect of SSI by comparing the seismic response of an isolated WST with that of two WST model. The two WST are identical and separated by a short horizontal distance, being coupled through the soil medium. The surface input excitation is the same for both comparative cases. The wave shadow effect (Xu et al., 1994) is visible in high frequency range. For the two WST coupled model there is a significant drop in the high frequency components from the bottom tank level to the surface due to the wave shadow effect. However for the bending moments in the tank shell the wave shadow effects appears to be less significant.

Figures 6 through 8 illustrates the results computed for a Reactor Building (RB) on a pile foundation in a relatively soft and liquefiable sand deposit (Ghiocel et al, 1996). Figure 6 shows the SASSI model of the RB including the pile foundation. Figure 7 shows the free-field liquefaction analysis results computed using an effective-stress computer program, LASS (Ghabousi and Dikmen, 1977-1984), and assuming the water table located just below ground surface. The liquefaction analyses indicated that there is a potential liquefiable sand layer between 1m and 6m depths. SSI analysis was performed using the equivalent soil properties computed from the free-field analysis assuming that limited liquefaction takes place between 1m and 6m depths. It was assumed that liquefaction starts at the beginning of the earthquake, and that it surrounds the pile foundation in all horizontal directions. The assumption is very drastic, so that the corresponding results represent an upper bound of the pile foundation response. As expected, the effect of liquefaction on pile forces was severe as illustrated in Figure 8. There is a major redistribution in the seismic forces and moments in the piles due to

liquefaction, which shows a large increase in the upper part of the piles, underneath basemat, where liquefaction occurred. It should be noted that the variability in the pile axial forces is larger than in the pile bending moments.

## PROBABILISTIC PREDICTION MODELS

Most of probabilistic seismic SSI analyses currently applied in practice, usually for critical facilities, use a lognormal format and base on simple technical guidelines such as those for the SPRA for NPP (Reed and Kennedy, 1994). These guidelines are a sort of modeling “recipes”, in which the effects of different SSI uncertainties are generically quantified. The bad part of such a simple approach is that the probabilistic modeling may be crude and that the quantified uncertainty effects given in guidelines are based on limited research investigations and measurements; so that may not reflect the particularity of a SSI problem. Because of this, such types of modeling “recipes” may impact sometimes negatively on the quality of a SSI prediction, especially when the particularity of the problem is significant. It should be understood that such simplified probabilistic approaches with questionable modeling simplifications, which were considered as feasible and versatile for practitioner engineers of the ‘80s, when the computational resources were low and probabilistic modeling was in infancy, should be replaced in the next future. Desirably, a probabilistic SSI analysis has to accurately determine, by itself, the effects of different uncertainties for a specific SSI problem and not to assume them. Several criticisms of the actual state-of-engineering practice are discussed in this section. Before doing this, a brief review of the lognormal format is presented (Kennedy et al., 1980).

### *Lognormal Format*

Lognormal format has been used extensively in the past two decades for developing seismic structural fragilities for critical facilities including SSI effects. At this time the lognormal format is the most popular probabilistic format in engineering practice. One of the main reasons for using

lognormal format for SPRA reviews is its mathematical simplicity for implementation. The lognormal distribution format is based on a mathematical expedience by combining subjective inputs with a multiplication scheme for fragility evaluation.

Using the lognormal format approach (Kennedy et al., 1980), a structural fragility curve which is a function of hazard parameter,  $A$ , is defined in terms of the median capacity,  $\tilde{A}$ , times the product of two random factors,  $\varepsilon_R$  and  $\varepsilon_U$ , representing the inherent randomness about the median value and the uncertainty in the median value as follows:

$$A = \tilde{A} \varepsilon_R \varepsilon_U \quad (1)$$

The two random factors are assumed to be lognormal random variables with median of unity and logarithmic standard deviation  $\beta_R$  and  $\beta_U$ , respectively. If there is no modeling uncertainty (only randomness) failure of probability as a function of hazard parameter is computed using the standard normal cumulative function  $\Phi(\cdot)$  by

$$P_f = \Phi\left[\frac{\ln(A / \tilde{A})}{\beta_R}\right] \quad (2)$$

If the modeling uncertainty is included then

$$P [p_f > p | A] = \Phi\left(\frac{\ln(A / A \exp[\beta \Phi^{-1}(p)])}{\beta_U}\right) \quad (3)$$

which computes the probability for which the failure probability  $p_f$  exceeds  $p$  given hazard parameter value  $A$  (Kennedy et al., 1980). Using the lognormal format, the probabilistic dynamic structural response for a hazard parameter reference level and probabilistic structural capacities are expressed as products of different factors (Kennedy et al., 1980, Reed and Kennedy, 1994). The basic two properties of lognormal model are (i) the median of a product of lognormal distributed random variables is equal to the product of the medians and (ii) the logarithmic standard deviation of a product is the square root of sum of squares of the individual logarithmic standard deviations.

In the early '80s, it has been considered by engineering experts that the accuracy of the probabilistic distribution in the region of fragility curve tails is not essential for a SPRA. Unfortunately, this is true only if the major risk contributors correspond to hazard parameter values far away from probability distribution tails, especially from the lower tail (Kennedy et al., 1980). More recently, comparative studies have indicated that the lognormal assumption for probability distribution applied in conjunction with multiplicative models for structural response and structural capacity may produce crude results for risk assessments (Hwang et al., 1987). In conjunction with the lognormal format, the use of a single reference level of the hazard parameter (assumed to be representative for the median structural capacity) for performing the SSI analysis, which has been applied in practice for expediency, may introduce significant inaccuracies. This is especially true when significant risk contributors come from random events defined by hazard parameters sensibly lower than reference level. A significant drawback of lognormal model is that the median capacity is insensitive to modeling uncertainty (Ellingwood, 1994).

One criticism of the lognormal format and its application based on the SPRA guidelines is related to probabilistic definition of seismic motion frequency content. As suggested by SPRA guidelines, the coefficient of variation of the spectral shape of a Uniform Hazard Spectrum (UHS) varies in the range of 0.25-0.30, which is typical for the Newmark-Hall spectrum type for the WUS, but less appropriate for the UHS type for the EUS. Figure 9 illustrate a typical UHS of a EUS NPP. It should be noted from this figure that the coefficient of variation of spectral shape varies in the range of 0.80-1.00, which is far larger than that recommended by the SPRA guidelines.

Another criticism is related to typical applications of the lognormal format in conjunction with SPRA guidelines for computing in-structure response spectra using the so-called "median output to median input" rule. This rule largely expedites the probabilistic SSI analysis, but introduces a significant modeling uncertainty due to the highly

nonlinear relationship between in-structure spectral peaks and the soil stiffness. This nonlinear relationship is shown in Figure 10. The use of a single deterministic SSI analysis for computing the median response for the reference level earthquake (other questionable concept for simplifying the probabilistic analysis) may introduce artificially high spectral peaks.

The last criticism discussed herein is related to the computation of the structural capacity using the lognormal format and the SPRA guidelines when significant SSI effects are present. The use of inelastic energy absorption factors computed using the methods suggested in the SPRA guidelines is drastically unconservative. Those methods are calibrated for fixed-base structure without SSI effects. If the fixed-base inelastic factors are combined with SSI results the overall safety margin is incorrectly estimated, as the inelastic absorption and SSI effects are not independent and their combination must take into account their dependencies. Otherwise, a double-counted margin is introduced. This should be avoided when the Newmark modified spectra method or the spectral averaging method derived for fixed-base structures are combined with SSI effects. The changes in natural frequencies and structural damping due to structural nonlinear effects have considerably less impact on a structural system having a large effective damping (including SSI energy radiation phenomenon), than on a fixed-base structure with low damping which is very sensitive to changes in its frequency and damping. Kennedy et al., 1985, based on a limited number of cases, gives two different expressions for the median inelastic factor,  $F_\mu$ :

$$F_\mu \approx \sqrt{0.6(\mu_s - 1) + 1} \quad \text{for fixed-base structures} \quad (4)$$

$$F_\mu \approx \sqrt{0.2(\mu_s - 1) + 1} \quad \text{including SSI (valid for a stiff soil)} \quad (5)$$

where  $\mu_s$  is the story drift ductility factor. For example, for a story ductility factor  $\mu_s=5.0$  the inelastic absorption factor is 1.8 for fixed-base cases and only 1.3 for SSI cases. For a NPP structure

founded on a softer soil the difference is obviously larger. Further research on this important aspect is needed.

The above criticisms are only a few of the many possible criticisms and, probably not the severest ones against the current state-of-engineering practice for probabilistic SSI analysis, more specific for NPP practice. These methodological deficiencies can be improved if the lognormal format is applied in conjunction with extensive simulations using random sampling techniques. This implies significant higher costs of probabilistic SSI analysis due to larger computational and human effort. It also requires highly qualified engineers on both SSI modeling and probabilistic modeling. A cost-effective alternative is to use specialized computer programs with user friendly interface for performing probabilistic SSI. In this idea, a probabilistic approach is proposed in this section (Ghiocel and Ghanem, 1999). This approach was recently implemented and applied in conjunction with SASSI models for SSI computations.

The above discussions suggest the need of a case-by-case type of probabilistic SSI methodology and computational tool, capable of including the particularity of a SSI problem. Specifically, SSI effects coming from deep embedment, structure-soil-structure interaction, motion incoherency for large size foundations, local soil instability should be more carefully considered in engineering practice. As shown in this paper each of these effects may significantly affect seismic SSI response.

### *Proposed Approach*

The most extensive studies performed in the past on probabilistic (seismic) SSI, which were supported by Nuclear Regulatory Commission (NRC), are those performed by Lawrence Livermore National Laboratory (LLNL, Shieh et al., 1985) and by Brookhaven National Laboratory (BNL, Pires et al., 1985). The LLNL study was based on a large number of case studies with the aim of identifying the most significant variables for seismic SSI effects and their influence on structural response variability. However, the LLNL study did not involve any probabilistic methodology. The

BNL study focused on nuclear containment structures using linear random vibration theory to calculate limit state probabilities under random seismic loads. The BNL departed from the current format suggested by the SPRA guidelines for NPP (Reed and Kennedy, 1994). However, the BNL methodology is restricted to superficial rigid circular foundations on a visco-elastic half-space. For realistic situations including arbitrary shaped and/or flexible foundations, partially embedded or buried structures, oblique seismic waves, non-uniform soil layering the BNL methodology is not directly applicable. The proposed probabilistic approach rigorously addresses these aspects.

A significant advantage of the proposed probabilistic approach is that the loads and system parameters can be more accurately described by random fields (time-space variability) rather than random variables (point variability) as assumed in the current SPRA reviews. Earthquake motion and soil properties are properly represented by random fields (Ghiocel, 1996, Ghiocel et. al 1996).

The key idea of the proposed approach is to provide a global complete description of the stochastic system response surface. The proposed approach has two implementation steps. The first step involves an expeditious condensation of the basic random processes via the KL expansion. The second step evaluates the coefficients of a stochastic orthogonal polynomial expansion of system response. After the coefficients of polynomial expansion are obtained, simulation of points on the system response surface can be obtained. Finally, probabilistic structural risks can be directly evaluated once the expansion of stochastic response surface is calculated.

Using Karhunen-Loeve (KL) expansion (Loeve, 1977, Ghanem and Spanos, 1991) a continuous random property field,  $p(\mathbf{x},\theta)$ , is expanded according to equation

$$p(\mathbf{x},\theta) = \sum_i \xi_i(\theta)p_i(\mathbf{x}) \quad (6)$$

where  $\theta$  denotes the random dimension,  $p_i$  represents a certain scale of fluctuation of the field  $p$  while  $\xi_i$  represents its random magnitude and hence

the random contribution of that particular scale to the overall property field. Both the property field and its various scales are global quantities and depend on the spatial position  $\mathbf{x}$ , they can also be multi-variate quantities. In the case where the material property in question is a random variable, the above sum is reduced to a single term.

The KL expansion of a stochastic process  $e(\mathbf{x},\theta)$ , is based on the spectral expansion of its covariance function  $R_{ee}(\mathbf{x},\mathbf{y})$ . Here,  $\mathbf{x}$  and  $\mathbf{y}$  are used to denote spatial coordinates, while the argument  $\theta$  indicates the random nature of the corresponding quantity. The covariance function being symmetrical and positive definite, by definition, has all its eigenfunctions mutually orthogonal, and they form a complete set spanning the function space to which  $e(\mathbf{x},\theta)$  belongs. It can be shown that if this deterministic set is used to represent the process  $e(\mathbf{x},\theta)$ , then the random coefficients used in the expansion are also orthogonal. The expansion then takes the following form

$$e(\mathbf{x},\theta) = \bar{e}(\mathbf{x}) + \sum_{i=1}^{\infty} \sqrt{\lambda_i} \xi_i(\theta) \phi_i(\mathbf{x}) \quad (7)$$

where  $\bar{e}(\mathbf{x})$  denotes the mean of the stochastic process, and  $\{\xi_i(\theta)\}$  form a set of orthogonal random variables. Furthermore,  $\{\phi_i(\mathbf{x})\}$  are the eigenfunctions and  $\{\lambda_i\}$  are the eigenvalues, of the covariance kernel, and can be evaluated as the solution to the following integral equation

$$\int_{\Delta} R_{ee}(\mathbf{x},\mathbf{y}) \phi_i(\mathbf{y}) d\mathbf{y} = \lambda_i \phi_i(\mathbf{x}) \quad (8)$$

where  $\Delta$  denotes the spatial domain over which the process  $e(\mathbf{x},\theta)$  is defined. The most important aspect of this spectral representation is that the spatial random fluctuations have been decomposed into a set of deterministic functions in the spatial variables multiplying random coefficients that are independent of these variables. The closer a process is to white noise, the more terms are required in its expansion, while at the other limit, a random variable can be represented by a single term. In physical systems, it can be expected that material

properties vary smoothly at the scales of interest in most applications, and therefore only a few terms in the KL expansion can capture most of the uncertainty in the process. It should be noted that in comparison with other series representations, the KL expansion has the minimum number of terms, or in other words the minimum number of random variables for random field decomposition.

For seismic SSI problems, of a particular interest are positive random fields, such as the amplitude of as a function of frequency or soil stiffness and hysteretic damping profiles as functions of depth, which are positive quantities. Thus, a new development consisting of a transformed space KL expansion was used for representing the positive non-normal random fields. The basis of this development is to find a mapping between the positive non-normal random field and an associated normal random field (Grigoriu, 1997). In particular, the treatment of lognormal processes is particularly expeditious given a number of analytic expressions that are available regarding it.

For SSI response, the covariance function is not known apriori, and hence the KL expansion cannot be used to represent it. Since the SSI solution process is a function of the material properties and seismic input, the entries of the nodal response vector  $\hat{\mathbf{c}}$  can be formally expressed as a nonlinear functional of a set  $\{\xi_i(\theta)\}$  used to represent the material and seismic input stochasticity. It has been shown that this functional dependence can be expanded in terms of polynomials in gaussian random variables, referred to as Homogeneous (or Polynomial) Chaoses (Cameron, 1947).

The expansion of SSI response takes on the following form (Ghanem and Spanos, 1991):

$$u(\mathbf{x},t,\theta) = a_0(\mathbf{x},t)\Gamma_0 + \sum_{i_1=1}^{\infty} a_{i_1}(\mathbf{x},t)\Gamma_1(\xi_{i_1}(\theta)) + \sum_{i_1=1}^{\infty} \sum_{i_2=1}^{i_1} a_{i_1 i_2}(\mathbf{x},t)\Gamma_2(\xi_{i_1}(\theta), \xi_{i_2}(\theta)) + \dots \quad (9)$$

In this equation, the symbol  $\Gamma_n(\xi_{i_1}, \dots, \xi_{i_n})$  denotes the Homogeneous (or Polynomial) Chaos (Kallianpur, 1980, Wiener, 1938) of order  $n$  in the variables  $(\xi_{i_1}, \dots, \xi_{i_n})$ .

Introducing a one-to-one mapping to a set with ordered indices denoted by  $\{\psi_i(\theta)\}$  and truncating the Homogeneous (or Polynomial) Chaos expansion after the  $p^{\text{th}}$  term, equation 10 can be rewritten as

$$u(\mathbf{x}, t, \theta) = \sum_{j=0}^p u_j(\mathbf{x}, t) \psi_j(\theta) \quad (10)$$

These polynomials are orthogonal in the sense that their inner product  $\langle \psi_j \psi_k \rangle$ , which is defined as the statistical average of their product, is equal to zero for  $j \neq k$ . A complete probabilistic characterization of the solution process  $u(\mathbf{x}, t, \theta)$  is obtained once the deterministic coefficients  $u_j(\mathbf{x}, t)$  have been calculated. A given truncated series can be refined along the random dimension either by adding more random variables to the set  $\{\xi_i\}$  or by increasing the maximum order of polynomials included in the Homogeneous (or Polynomial) Chaos expansion. The first refinement takes into account higher frequency random fluctuations of the underlying stochastic process, while the second refinement captures strong non-linear dependence of the solution process on this underlying process (Ghanem and Spanos, 1991).

Using the orthogonality property of polynomials, the coefficients of the Homogeneous Chaos of the solution process can be computed by

$$u_k = \frac{\langle \psi_k u \rangle}{\langle \psi_k^2 \rangle} \text{ for } k = 1, \dots, K \quad (11)$$

One of the key factors for obtaining an efficient numerical implementation of the stochastic approach based on Homogeneous Chaos expansion is related to the computation of the inner products or averages  $\langle \psi_k u \rangle$  in equation 11. This can be rewritten in an explicit integral form

$$\langle \psi_k u \rangle = \int_{-\infty}^{\infty} \psi_k(\xi) u(\xi) \exp\left(\frac{1}{2} \xi^T \xi\right) d\xi \quad (12)$$

Polynomial Chaoses are orthogonal with respect to the Gaussian probability measure, which makes them identical with the corresponding

multidimensional Hermite polynomials (Grad, 1949). From the above equation it is obvious that the integration domains spans a large multidimensional space, the dimensionality being given by the number of elementary standard normal random variables defining the set  $\{\xi_i\}$ . The multidimensional integral given in equation (11) can be computed using various integration procedures including Gauss-Hermite quadrature or efficient simulation techniques. For actual integration an innovative stratified sampling technique was employed. An alternate approach using advanced stochastic finite element concepts is described elsewhere (Ghiocel and Ghanem, 1999).

For getting a faster convergence in the case of non-normal processes, a transformed space representation of non-normal processes was used. Therefore, a logarithmic transformation was applied at the level of the extreme responses before expanding it in a Homogeneous Chaos. Then the expansion was performed in a transformed space for which the corresponding process is closer to a normal process. Finally, the non-normal process was determined using an inverse transformation, specifically an exponential transformation. This transformation is expressed mathematically by

$$u = \exp\left(\sum_{i=1}^n \frac{\langle \ln(u) \psi_i \rangle}{\langle \psi_i^2 \rangle} \Psi_i\right) \quad (13)$$

This significantly has speeded up the convergence and has improved the accuracy of the computed series expansions for extreme-value responses.

### *Earthquake Motion Description*

Earthquake ground acceleration was represented by a segment of a (non)stationary random process (nonstationarity was introduced by using a deterministic intensity shape function) with zero mean, known frequency content and spatial correlation structure. This stochastic representation is conditional to the given zero-period peak ground acceleration (ZPGA) level. For evaluation of the overall seismic structural risk all the ZPGA levels, i.e. the seismic hazard curve at the site, should be

considered. For each ZPGA level, the frequency content of earthquake motion is described locally, in a point at ground surface, by either a acceleration probabilistic response or a power spectral density function. The three earthquake motion components were assumed to be statistically independent. The spatial correlation structure of ground motion field, which is a function of frequency, was defined by a coherency spectrum matrix.

*Local (Point) Description:* Typically in engineering practice probabilistic site-specific ground response spectra were defined for hazardous facilities (LLNL, 1993, EPRI, 1991). The probabilistic ground spectra are usually described by three digitized spectral response curves computed for 15%, 50% and 85% non-exceedance probability assuming a lognormal distribution of amplitudes. Herein, the probabilistic ground spectrum was assumed as an one-dimensional lognormal random field in frequency domain with certain bandwidth characteristics given by the soil deposit behavior as a second-order linear filter for incoming seismic waves. The spectral amplitude field was modeled by a lognormal random field using a transformed KL expansion. As an alternate of local description of earthquake ground motion, the power spectral density may be input instead of a probabilistic spectra. Four analytical expressions were considered for the power spectral density (Pires et al., 1985):

- (i) Kanai-Tajimi spectrum (spectral shape similar to the acceleration transfer function of single degree of freedom subjected to a base excitation)

$$S(\omega) = \frac{1 + 4\xi_f^2 (\omega / \omega_f)^2}{[1 - (\omega / \omega_f)^2]^2 + 4\xi_f^2 (\omega / \omega_f)^2} \quad (14)$$

- (ii) Ruiz-Penzien spectrum

$$S(\omega) = \frac{1 + 4\xi_f^2 (\omega / \omega_f)^2}{[1 - (\omega / \omega_f)^2]^2 + 4\xi_f^2 (\omega / \omega_f)^2} \frac{(\omega / \omega_p)^4}{[1 - (\omega / \omega_p)^2]^2 + 4\xi_p^2 (\omega / \omega_p)^2} \quad (15)$$

- (iii) Ruiz-Penzien spectrum multiplied by a low-pass first-order filter and

$$S(\omega) = \frac{1 + 4\xi_f^2 (\omega / \omega_f)^2}{[1 - (\omega / \omega_f)^2]^2 + 4\xi_f^2 (\omega / \omega_f)^2} \frac{(\omega / \omega_p)^4}{[1 - (\omega / \omega_p)^2]^2 + 4\xi_p^2 (\omega / \omega_p)^2} \frac{1}{1 + L^2 \omega_q^2} \quad (16)$$

- (iv) Brookhaven National Lab (BNL) spectrum

$$S(\omega) = S_0 \sum_{j=1}^2 P_j \frac{(1 + 4\xi_j^2)[1 - \exp(-\omega^4 / \omega_j^4)]}{[1 - (\omega / \omega_j)^2]^2 + 4\xi_j^2 (\omega / \omega_j)^2} \quad (17)$$

where  $\omega_f, \omega_p$  and  $\xi_f, \xi_p$  are the frequency and bandwidth of the filters.

These analytical forms are widely accepted by the earthquake engineering community, being the most popular ones. The Kanai-Tajimi spectrum, (i), was the first of the above expression to be proposed. The Ruiz-Penzien spectrum, (ii), was intended to adjust the low frequency content of Kanai-Tajimi spectrum at frequency equal to zero. The improved Ruiz-Penzien spectrum, (iii), reduces the high frequency content of the Kanai-Tajimi spectrum. The BNL spectrum, (iv), has a lower high frequency content than the Kanai-Tajimi spectrum removes the singularity of the displacement spectral power density at zero frequency (Pires et al., 1985).

*Spatial Variation (Incoherency):* For an incoherent wave field the unlagged coherence for two point motions i and k can be defined as (Abrahamson et al, 1990):

$$\text{Coh}_{U_{i,k}}(\omega) = \text{Coh}_{i,k}(\omega) A(i\omega, X_i - X_k) \exp [i\omega(X_i - X_k) / V_{xi-xk}] \quad (18)$$

where  $A(i\omega, X_i - X_k)$  is a decaying function of frequency starting from unit value which gives the relative power of the wave field described by a plane wave at all frequencies. The term  $\exp[i\omega(X_i - X_k) / V_{xi-xk}]$  in equation 23 represents in the frequency domain the phase angle between the two point motions due to the wave passage effect. Parameter  $V_{xi-xk}$  is the apparent seismic wave velocity defined by the distance between the

two points, absolute of  $X_i - X_k$ . If the wave field is perfectly described by a single plane wave, the function  $A(i\omega, X_i - X_k)$  is equal to unity.

For two one-dimensional random time series representing an unidirectional seismic motion components in two arbitrary points of the soil deposit,  $j$  and  $k$ , the (narrow band) coherence is defined by a complex function of frequency

$$\text{Coh}_{j,k}(\omega) = \frac{S_{j,k}(\omega)}{[S_{j,j}(\omega)S_{k,k}(\omega)]^{1/2}} \quad (19)$$

where  $S_{j,k}(\omega)$  is the cross-spectral density function for two points  $j$  and  $k$ , and  $S_{j,j}(\omega)$  is the auto-spectral density for point  $j$  (similar for point  $k$ ). The coherence describes the similarity of the two point motions. Generally, in engineering applications, the so-called “lagged” coherency spectrum or “lagged” coherence are used (Abrahamson et al., 1990). The lagged coherency includes only the amplitude randomness and removes the wave-passage randomness. From physical point of view, the lagged coherence represents the fraction of the total power of seismic motion which can be idealized by a single deterministic plane wave motion called the coherent motion. Usually in the current earthquake engineering language, the lagged coherence is called simply coherence. More generally than the “lagged” coherence, the “unlagged” coherence includes the wave-passage random effects.

Based on the experimental evidence of different records of past earthquakes, the following analytical forms for the coherence function were considered:

(i) Luco-Wong model (Luco and Wong, 1986), defined by

$$\text{Coh}_{i,k}(\omega) = \text{Coh}(|X_i - X_k|, \omega) = \exp[-(\gamma|X_i - X_k|/V_s)^2] \quad (20)$$

in which  $\gamma$  is the coherence parameter and  $V_s$  is the shear wave velocity in the soil. The above analytical expression compared with others given in the

technical literature based on experiment fitting (Hoshiya and Ishii, 1983, Harichandran and Vanmarcke, 1986, etc.) has the advantage of a theoretical support based on the analytical formulation of shear wave propagation in random media (Uscinski, 1977). Luco and Wong, 1986, suggested that the coherence parameter has generic values in the range of 0.10 to 0.30.

(ii) Abrahamson model (Abrahamson, 1991, 1993), defined by

$$\text{Coh}_{i,k}(\omega) = \text{Coh}(|X_i - X_k|, \omega) = \text{Tanh}\{(a_1 + a_2|X_i - X_k|)[\exp[-(b_1 + b_2|X_i - X_k|)\frac{\omega}{2\pi}] + \frac{1}{3}(\frac{\omega}{2\pi})^{-c}] + k\} \quad (21)$$

where  $a_1$ ,  $a_2$ ,  $b_1$ ,  $b_2$  and  $c$  are model parameters. These parameters can be introduced by the user, otherwise by default the values (Abrahamson, 1990) are used, i.e.  $a_1=2.55$ ,  $a_2=-0.012$ ,  $b_1=0.115$ ,  $b_2=0.00084$ ,  $c=0.878$  and  $k=0.35$ . These parameters may be defined as random variables.

Assuming that the seismic wave field can be modeled by a plane wave, an element of the cross-spectral density matrix of multidimensional motion random field can be derived analytically

$$S_{i,k}(\omega) = [S_{i,i}(\omega)S_{k,k}(\omega)]^{1/2} \text{Coh}(|X_i - X_k|, \omega) \exp[i\omega(X_i - X_k)/V_{X_i - X_k}] \quad (22)$$

for each pair  $i,k$  of point motions.

To implement the random field model of incoherent soil motion, the coherence matrix is decomposed via KL expansion. The motion incoherency effects are larger for higher frequency components than for lower frequency components. Usually, the effect of incoherency is to reduce translational motion and rocking motion and increase torsional motion.

#### *Soil Property Description*

Soil properties were assumed to be homogeneous in a horizontal plane and therefore they were idealized as one-dimensional random fields, i.e. random varying profiles with depth.

Specifically, the randomness in soil dynamic properties was considered by variabilities in shear modulus, hysteretic damping and Poisson ratio. First, the soil deposit was discretized in a geometric layering with varying properties. Soil shear modulus at low strains,  $G_{\max}$ , was idealized as an one-dimensional lognormal random field in the vertical direction having a non-stationary mean and an assumed correlation length for same material type. This idealization is considered to be significantly more realistic and less conservative than the assumption of perfect correlation currently applied for parametric deterministic SSI studies. For soil layering including different materials, a set of multiple random fields may be considered. The shape (nondimensional variation) of the shear modulus - shear strain curve,  $G(\gamma)/G_{\max} - \gamma$  was modeled by a random field along the shear strain axis with a non-stationary mean. The mean curve was assumed to have an arbitrary shape which is either introduced by the user or by default stored in the program database. The same modeling assumption used for the shear modulus curve was considered for the hysteretic damping - shear strain curve,  $D(\gamma)$ .

For implementation, the soil property fields were decomposed via KL expansion. The statistics of the soil property field models, including correlation length parameters, were derived by calibrating the mathematical models with experimental data available.

### *Structural Properties*

Structure damping and stiffness parameters were assumed to be random variables. This assumption is based on the fact that the random variation of these parameters within the superstructure are appropriately a set of independent random variables, than by a continuous random field with a well-established correlation structure expandable in a KL series.

### *Example Application*

The proposed approach was applied to a typical Reactor Building (RB) subjected to earthquake motion. The probabilistic SSI response was

compared with a deterministic SSI response computed using the current practice for NPP. The finite element model used for seismic soil-structure interaction analysis is shown in Figure 11 (Lysmer et al., 1988). This SSI computational model represents a typical SASSI model for seismic design basis calculations of a reactor building. The superstructure is modeled by beam elements and the basemat is modeled by solid elements. Rigid links are introduced to transmit the rocking motion from the superstructure stick to the basemat. The ACS SASSI computer program (Ghiocel, 1997) was used for both the free-field analysis and the SSI analysis, performed either probabilistically or deterministically.

Deterministic analysis was done for a seismic input defined by the design ground spectrum associated to a 84% probability of nonexceedance. A spectrum compatible accelerogram was generated for SSI analyses. As shown in Figure 12 the computed response spectra of the generated accelerogram slightly envelopes the given design spectrum. Soil properties were be the best-estimate values (median). In accordance to the current seismic design requirements, two additional extreme bounds, 0.50 times best-estimate and 2.00 times best-estimate values were considered. The final results of the deterministic analysis are obtained by enveloping the results for the three soil-structure interaction analysis for the three set of values of soil parameters.

For probabilistic analysis, the earthquake input was defined by a probabilistic response ground spectrum as shown in Figure 13. The four spectral curves corresponds to mean, median and 16% and 85% nonexceedance probability estimates. The probability distribution was assumed to be lognormal. The lognormal spectral amplitude field was represented using a transformed KL expansion. The correlation length along frequency axis was selected depending on the desired bandwidth of simulated spectra (function of damping). The number of frequency steps to describe the spectral shape was 100. The smaller the correlation length is, the narrower the spectral peaks are. Figure 14 illustrates the ensemble statistics (for nonexceedance probabilities of 15%, 50%, 85% and mean) of the probabilistic model of ground response

spectrum for a set of 100 realizations. Few simulated realizations are shown in Figure 15. For probabilistic soil-structure interaction analysis the effect of motion incoherency was considered using a Luco-Wong model with a  $\gamma$  parameter of 0.20. The resulted spatial variation of motion amplitude for different frequencies is plotted in Figure 16.

Soil properties were defined assuming that the low strain soil shear modulus and hysteretic damping profiles (variation with depth) are lognormal random fields. Figure 17 shows the probabilistic shear modulus profile (statistically estimated profiles are included). Plotted curves correspond to mean, median and 16% and 84% nonexceedance probability. A transformed space KL expansion was used to represent these lognormal positive fields. The variation of nondimensional shear modulus and hysteretic damping versus shear strain were modeled as normal random fields decomposable directly in original space in KL expansion. Simulated variations are shown in Figure 19.

Structural properties are described using random variables. Specifically, the Young elastic modulus and the material damping ratio were assumed to be normal random variables with a coefficient of variation of 0.25. The means were assumed to be 0.80 of the linear elastic modulus and 8%, respectively.

A comparison of probabilistic response computed using the proposed approach (using 100 solutions) and a Monte Carlo simulation (using 500 solutions) is shown in Figure 20.

Figure 21 shows the coefficients of the transformed Homogeneous Chaos expansion using 72 basic random variables. Between 1 and 72 are the coefficients of the first-order polynomials, and between 73 and 144 are the coefficients of the second-order polynomials (without coupling). It is to be noted that only less than half of the number of basic random variables have significant contributions. Larger contributions come from linear terms than from nonlinear terms. However, it is very difficult for the complex soil-structure problem to preliminary establish with are the most significant variables. There is a need to get more insights on this aspect in the future.

Figure 22 shows a comparison between deterministic and probabilistic analysis results, both in terms of in-structure response spectra. Deterministic estimates corresponds to very low nonexceedance probability levels. Having in mind the additional conservatism introduced in the overall seismic evaluation by the seismic hazard definition and the evaluation of structural elements or equipment capacities, it appears that the current deterministic SSI analysis procedure is overly conservative.

## CONCLUDING REMARKS

The paper addresses the effects of SSI modeling uncertainty on seismic response, discusses shortcomings of current state-of-engineering practice on probabilistic SSI for hazardous facilities, and proposes a new accurate procedure for performing probabilistic SSI analysis. SSI modeling uncertainty effects are illustrated using the results from different case studies. The proposed procedure represents a significant advancement for performing probabilistic seismic SSI analyses of hazardous facilities.

The proposed approach based on a stochastic series representation of SSI response offers accuracy, efficiency and significant modeling advantages in comparison with the currently SPRA approaches. The proposed approach addresses efficiently large number of variables problems such as dynamic SSI problems and handles random field models, useful for idealization of dynamic loading and system parameters. In addition, the proposed approach is capable of handling large variability and highly nonlinear problems.

## ACKNOWLEDGEMENTS

The paper is partially based upon work supported by the National Science Foundation under a SBIR project with the Award Number DMI-9660321.

## SELECTED REFERENCES

Abrahamson, N. A. et al. (1990). Spatial Variation of Strong Ground Motion for Use in Soil-

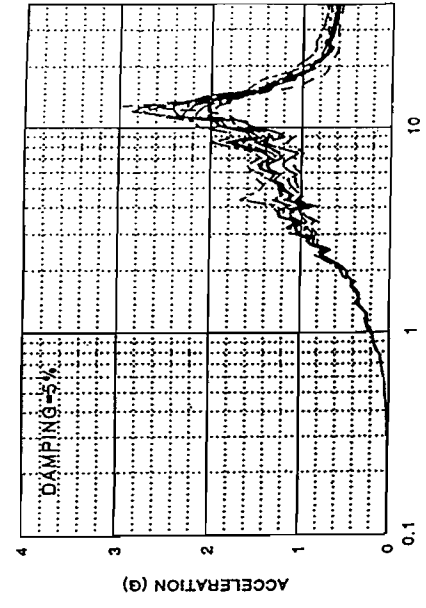
- Structure Interaction Analyses, *4th U.S. National Conference on Earthquake Engineering, Palm, Springs, Vol.1.*
- Cameron, R. and Martin W (1947). The Development of Nonlinear Functionals in Series of Fourier-Hermite Functionals, *Ann. Math.*, 48, 385-392.
- EPRI (1989). Probabilistic Seismic Hazard Evaluation at Nuclear Plant Sites in the Central and Eastern United States: Resolution of Charleston Issue, *Report NP-6395-D.*
- Ghaboussi, J. and Dikmen, S.U (1977). LASS II - Computer Program for Analysis of Seismic Response and Liquefaction of Horizontally Layered Sands, *Report UILU-ENG-79-2010.*
- Ghanem, R., Ghiocel, D.M.(1996). A Comparative Analysis of FORM/SORM and Polynomial Chaos Expansion for Highly Nonlinear Systems *ASCE/EMD Speciality Conference, Ft. Lauderdale.*
- Ghanem, R., and Spanos, P. (1991). Stochastic Finite Elements: A Spectral Approach, *Springer-Verlag.*
- Ghiocel, D. M. and Ghanem, R. (1999). A Stochastic Finite Element Approach for Seismic Soil-Structure Interaction, *Journal of Earthquake Engineering and Structural Dynamics*, *ASCE (submitted).*
- Ghiocel, D.M. and Ghanem, R. (1998). Stochastic Seismic SSI Using Homogeneous Chaos Expansion, *the 12th ASCE Engineering Mechanics Speciality Conference, San Diego, May.*
- Ghiocel, D.M. (1996) Seismic Motion Incoherency Effects on Dynamic Response, *7th ASCE EMD/STD Joint Speciality Conference on Probabilistic Mechanics and Structural Reliability, Worcester, MA, August.*
- Ghiocel, D.M. et al. (1996) Probabilistic Seismic Analysis Including Soil-Structure Interaction, *7th ASCE MD/STD Joint Speciality Conference on Probabilistic Mechanics and Structural Reliability, Worcester, MA, August.*
- Ghiocel, D. M. (1997) ACS SASSI/PC - An Advanced Computational Software for System Analysis of Soil-Structure Interaction on Personal Computers, *ACS Report, Cleveland, Ohio.*
- Ghiocel, D. M., Wilson, P., Stevenson, J. D., (1995). Evaluation of Probabilistic Seismic FRS Including SSI Effects, *the 13th SMIRT Conference, Invited Paper, Vol. M, Porto Alegre.*
- Ghiocel, D.M., et al., (1990) "Evaluation of SSI and SSSI Effects on Seismic Response of Nuclear Heavy Buildings by Different Approaches", *the 10th European Conference on Earthquake Engineering, Moscow.*
- Ghiocel, D. M., et al.,(1987) "Structural Reliability of Prestressed Concrete Nuclear Containment Under Combined Loads", *the 9th SMIRT, Vol. M, Lausanne.*
- Ghiocel, D. M.,(1986) "Probabilistic Seismic Soil-Structure Interaction Analysis", *8th ECEE Conference, Lisbon*
- Hwang et al. (1987). Seismic Probabilistic Risk Assessment for Nuclear Power Plants, *NCEER-BNL-Report 87-0011.*
- Kallianpur, G. (1980). Stochastic Filtering Theory, *Springer Verlag.*
- Kennedy, R.P, Cornell, C.A., Campbell, R.D., Kaplan, S., Perla, H.F. (1980). Probabilistic Seismic Safety Study of An Existing Nuclear Power Plant. *Nuclear Eng. & Des.*, Vol. 59.
- Kennedy, R.P., Kincaid, R.H., Short, S.A. (1985) . Engineering Characterization of Ground Motion. Task II, *NUREG/CR-3805, Vol. 2.*
- LLNL (1993) Eastern US Seismic Hazard Characterization Update, *Lawrence Livermore National Laboratory Report UCRL-ID-115111*
- Loeve, M.,(1948) Probability Theory, *McGraw-Hill.*
- Lysmer, J.,Tabatabaie-Raissi, Tajirian, F.Vahdani, S., and Ostadan, F.(1988), SASSI - A System for Analysis of Soil - Structure Interaction, Report UCB 1988, *Geotechnical Engineering, University of California, Berkeley.*
- Luco, J. and Wong, H. L. (1986). Response of a Rigid Foundation to a Spatially Random Ground Motion, *Earthquake Engineering & Structural Dynamics.*
- Miller, C.A. and Costantino, C.J. (1994). " Seismic Induced Pressures in Buried Vaults", *Natural Hazard Phenomena and Mitigation, ASME, PVP-Vol.217, p. 3-11.*

- Pires, J., Hwang, H., and Reich, M., (1985). Reliability Evaluation of Containments Including Soil-Structure Interaction, *USNRC Report NUREG/CR-4329, BNL-NUREG-5190.6*
- Reed, J.W., Kennedy, R.P. 1994. Methodology for Developing Seismic Fragilities.
- Shieh, L.C., et al. 1985. Simplified Seismic PRA: Procedures and Limitation, *NUREG/4331, UCID-20468*.
- Xu, J., Bandyopadhyay, K., Miller, C.A., Costantino, C.J. (1994) "Spacing Effects on Seismic Responses of Underground Waste Storage Tanks", *Natural Hazard Phenomena and Mitigation, ASME, PVP-Vol. 217*, p. 13-18.
- Wiener, N (1938). The Homogeneous Chaos, *Amer. J. Math.*, 60, p. 897-936.

DMG:jah

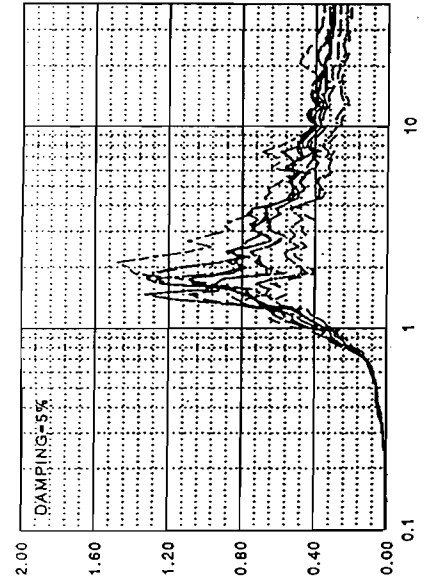
D:\ghiocel\ssiawk98.doc

AUXILIARY STRUCTURE-DIR.N-S- SIMULATIONS  
ELEVATION 117.5 FT. - EAST OF SF POOL



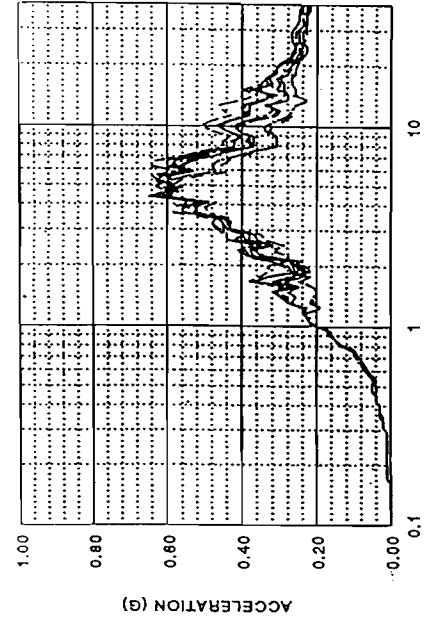
c) AB, roof level

CONTAINMENT SHELL - ELEVATION 163.0 FT



b) RB, top on containment

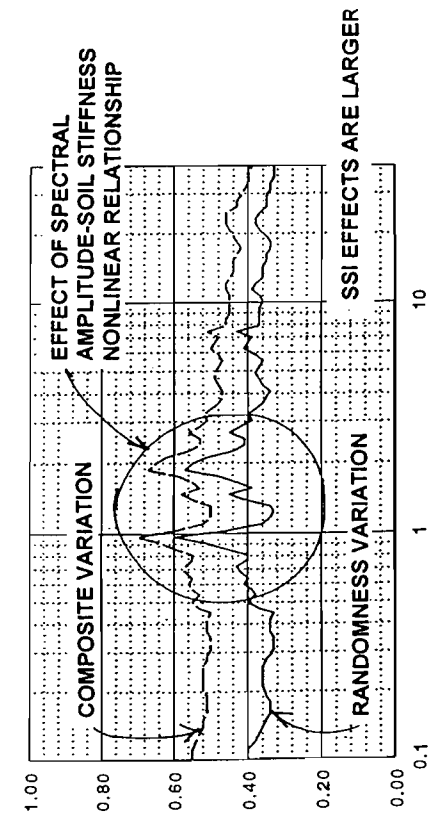
BASB MAT - ELEVATION 8.5 FT



a) RB, basemat

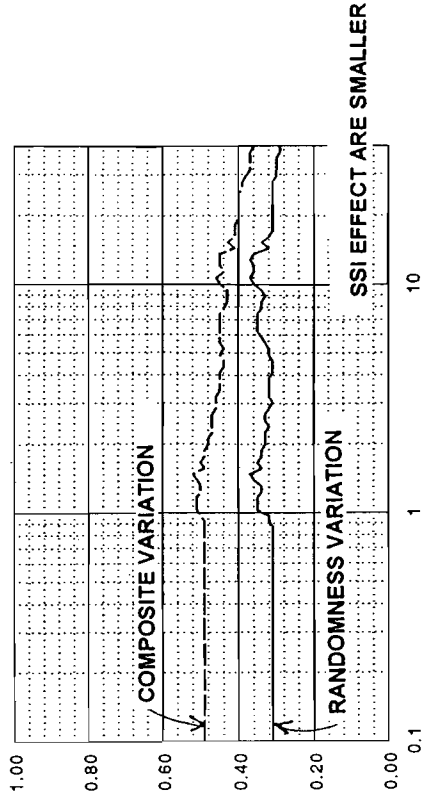
Figure 1. In-structure spectra in the RB and AB

CONTAINMENT SHELL - ELEVATION 163.0 FT



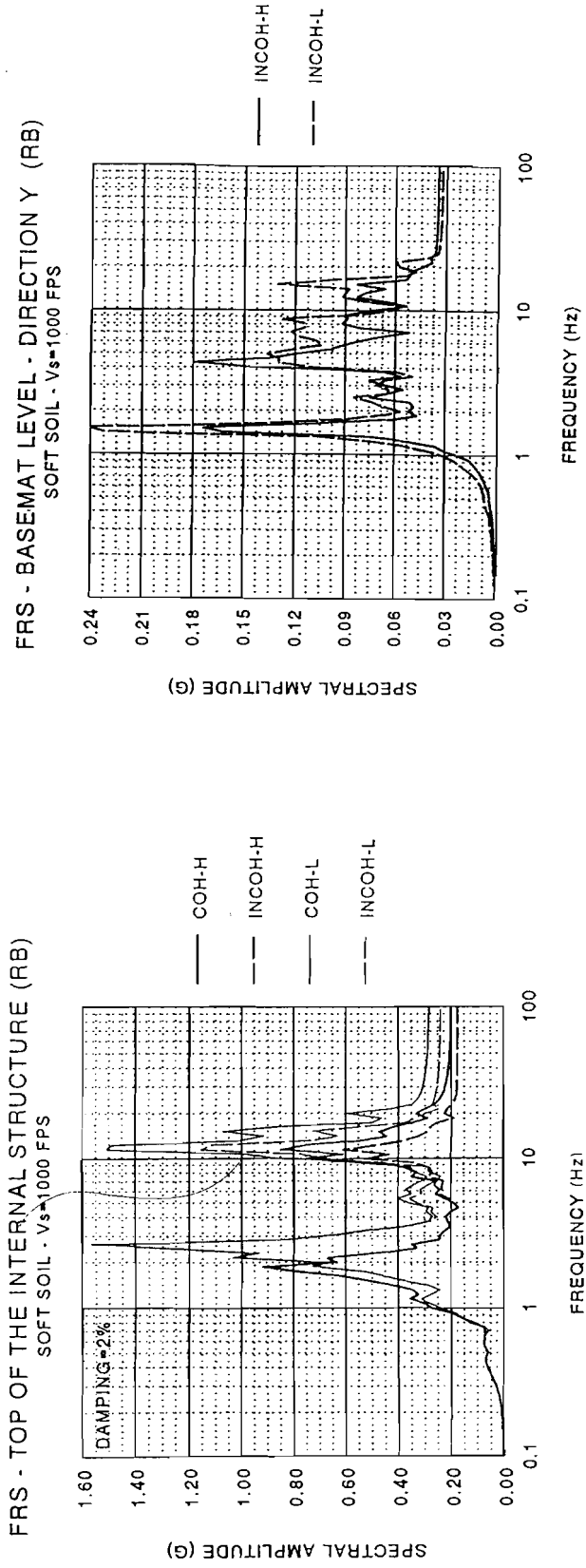
a) RB, top of containment

CONTAINMENT SHELL - ELEVATION 163.0 FT



b) AB, roof level

Figure 2. Coefficients of variation for the in-structure spectra



a) Top of internal structure, horizontal motion  
b) Basemat, torsional motion

Figure 3. Effect of incoherency on in-structure spectra

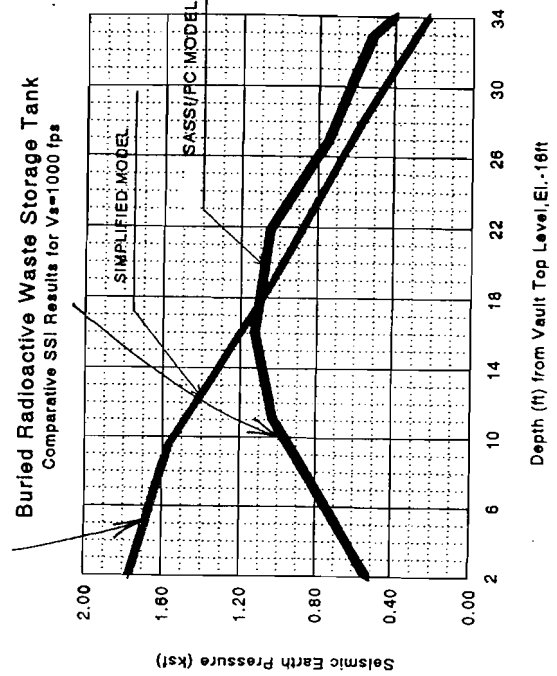
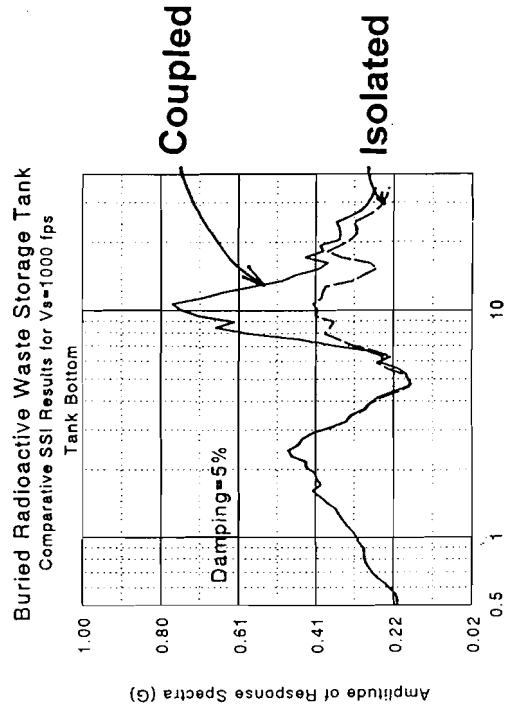
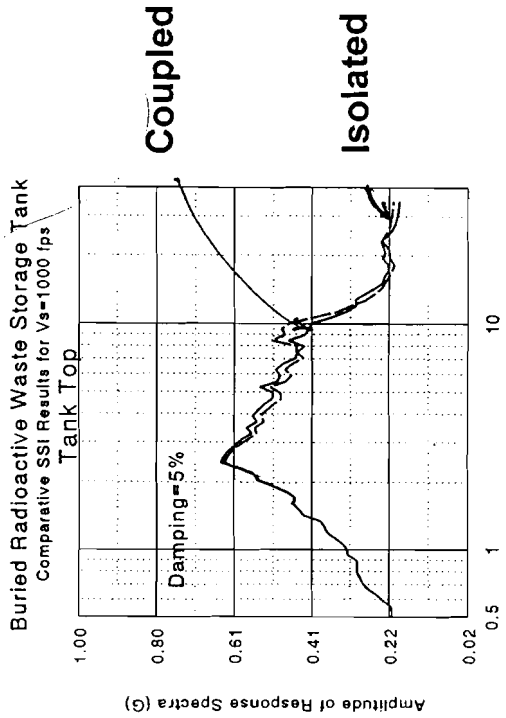


Figure 4. Seismic pressure on WST wall



a) Surface motions



b) Bottom tank motions

Figure 5. Response spectra for the WST model

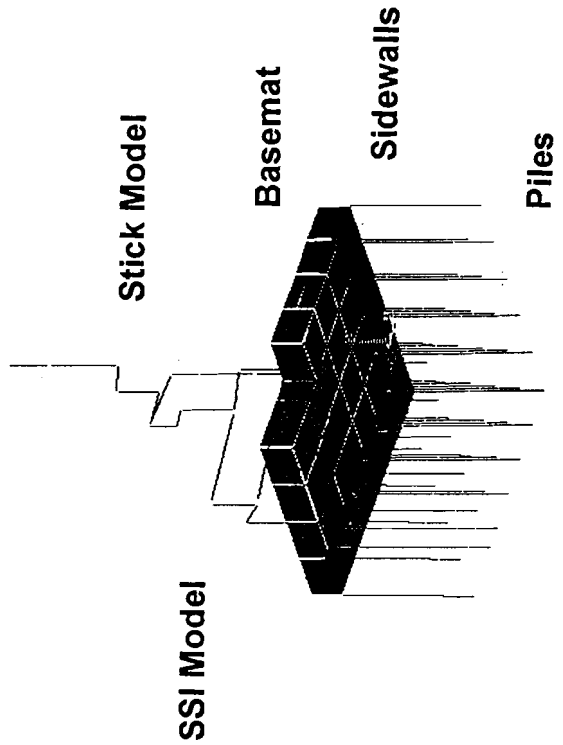


Figure 6. Structure-pile foundation SSI model

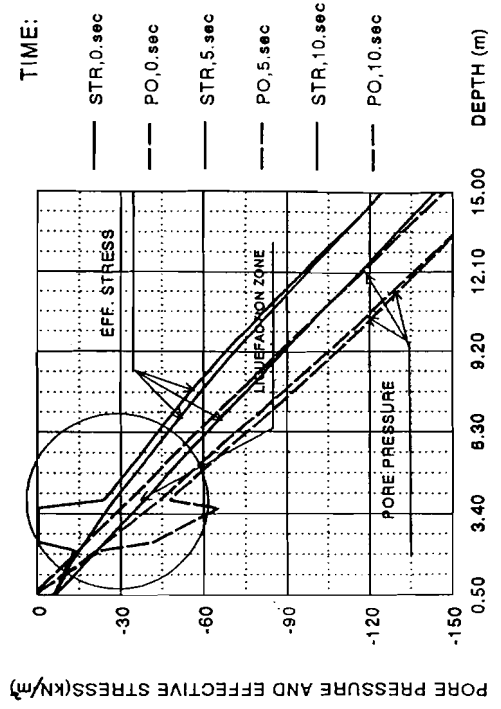


Figure 7. Pore pressure and effective stresses in soil

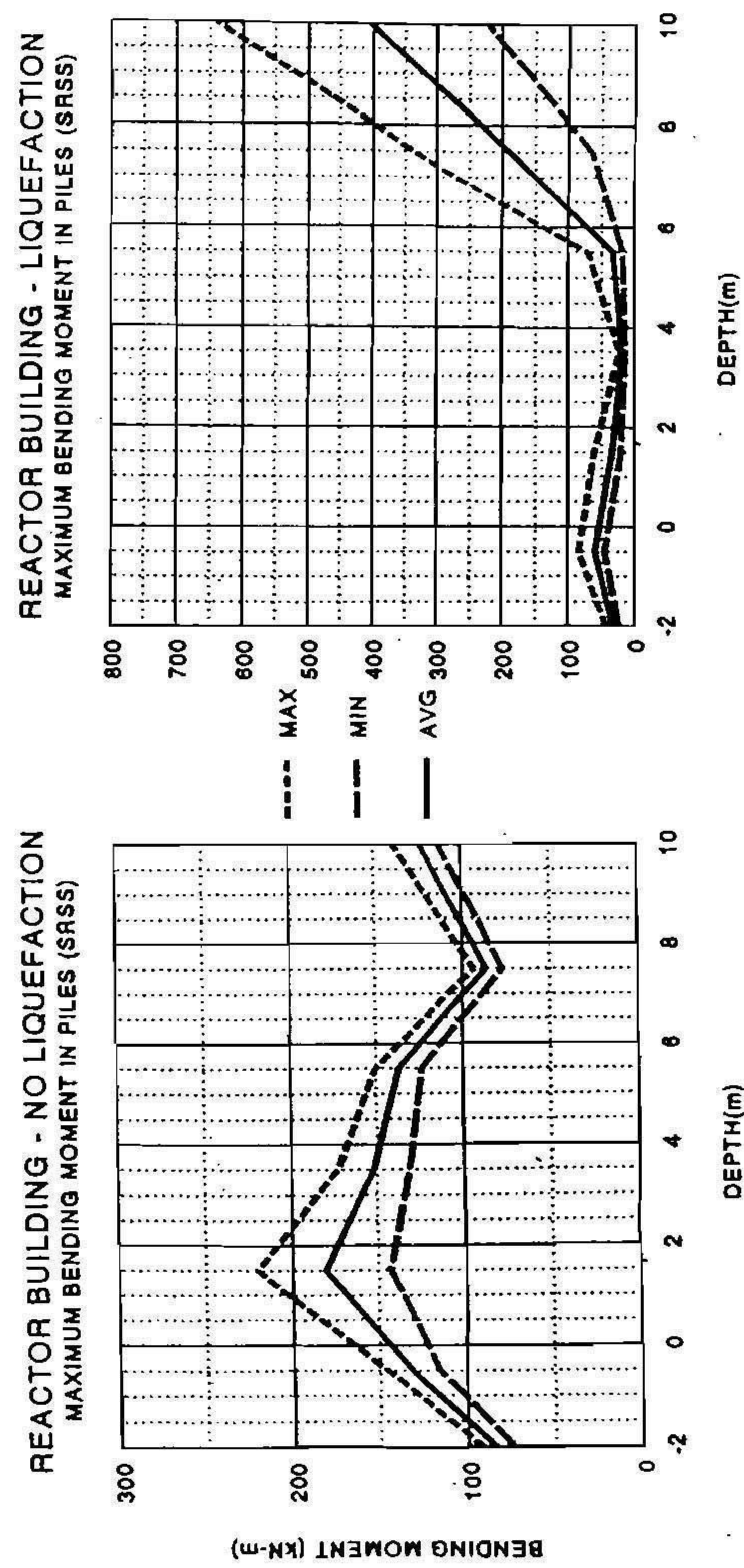
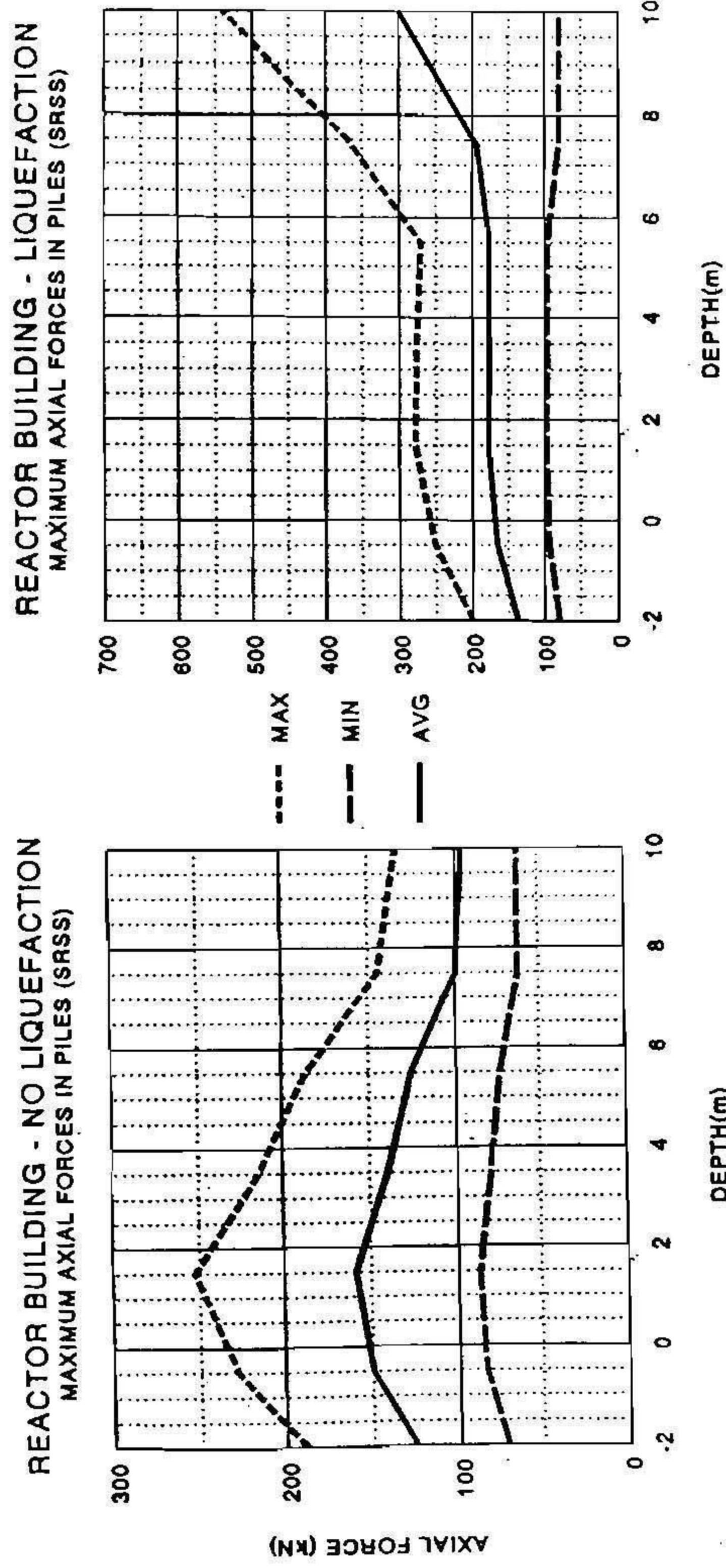


Figure 8. Forces and moments in piles

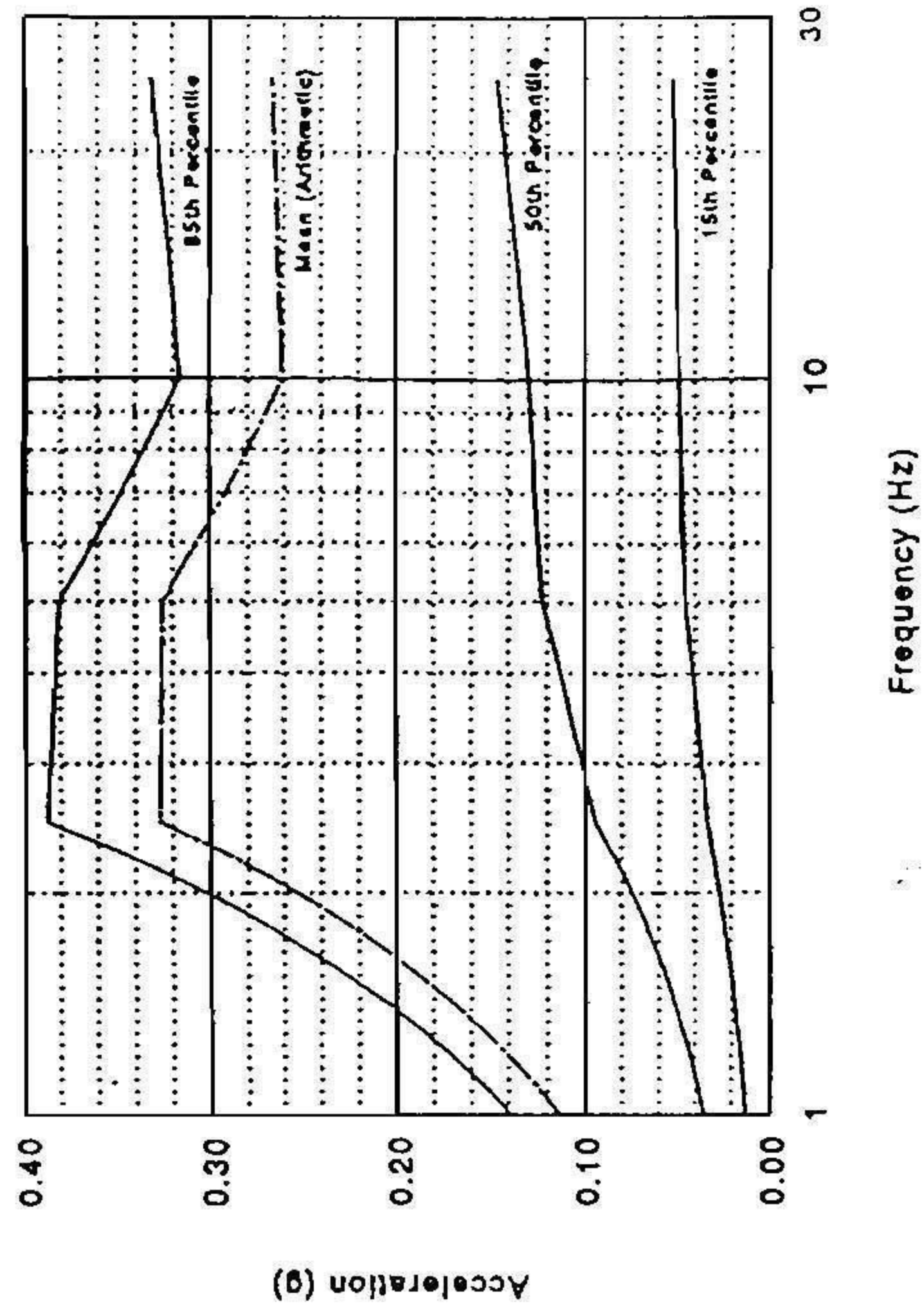


Figure 9. Typical UHS for a EUS NPP site

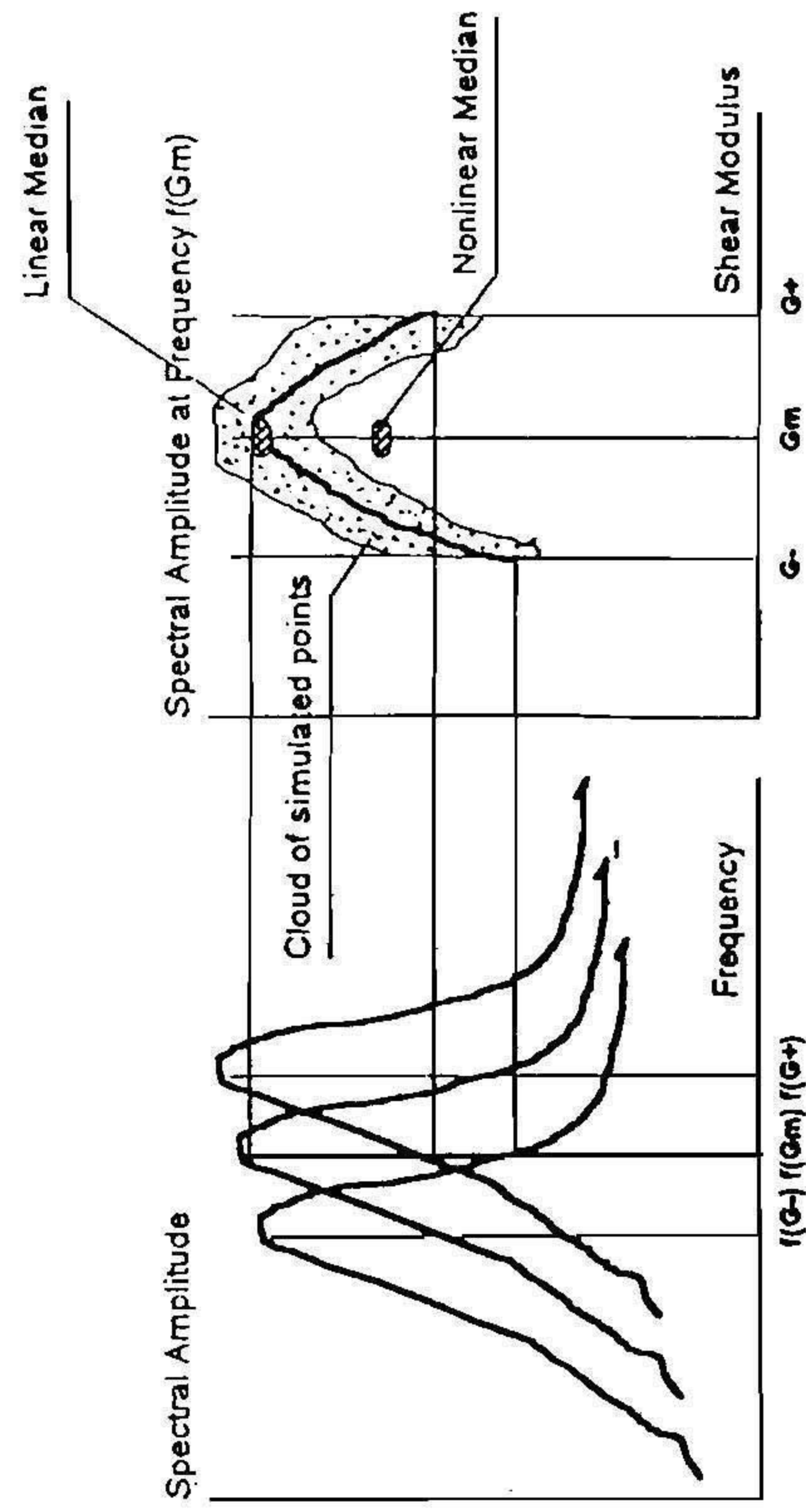


Figure 10. Highly nonlinear relationship between spectral peaks and soil stiffness

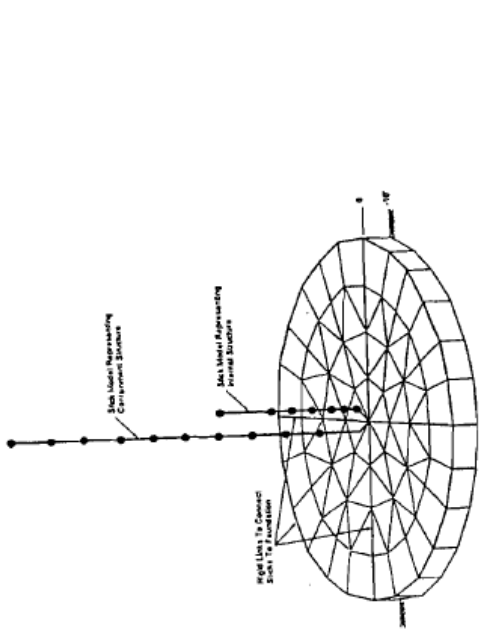


Figure 11. RB SSI model (after Lysmer et al., 1988)

PROBABILISTIC GROUND SPECTRUM (Damp. = 5%)

Statistical Estimations - Logn. Distrib.

— MEAN ——— MEDIAN - - - - 16% - - - - 84%

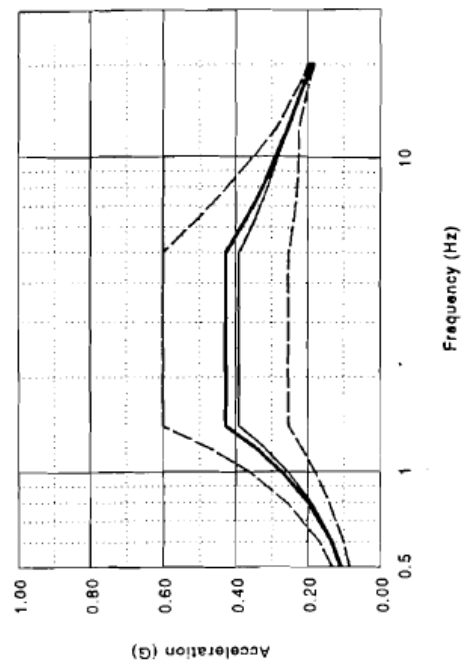


Figure 13 Probabilistic ground response spectra

DETERMINISTIC (DESIGN) GROUND SPECTRUM

ZPGA=0.20g, Damping=5% - 84% Probability

— COMPUTED ——— DESIGN

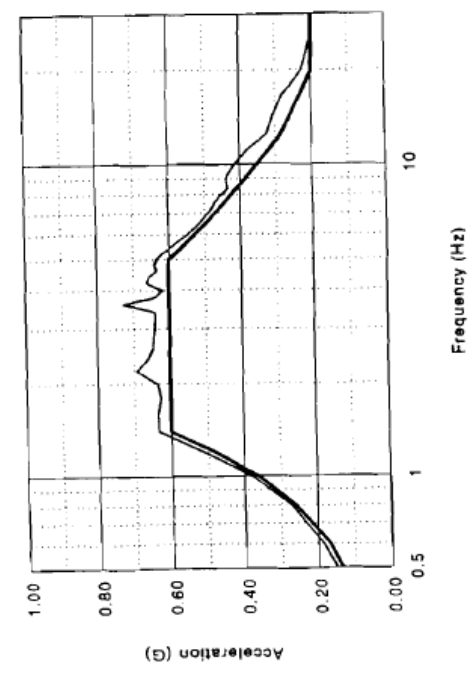


Figure 12 Deterministic ground response spectra

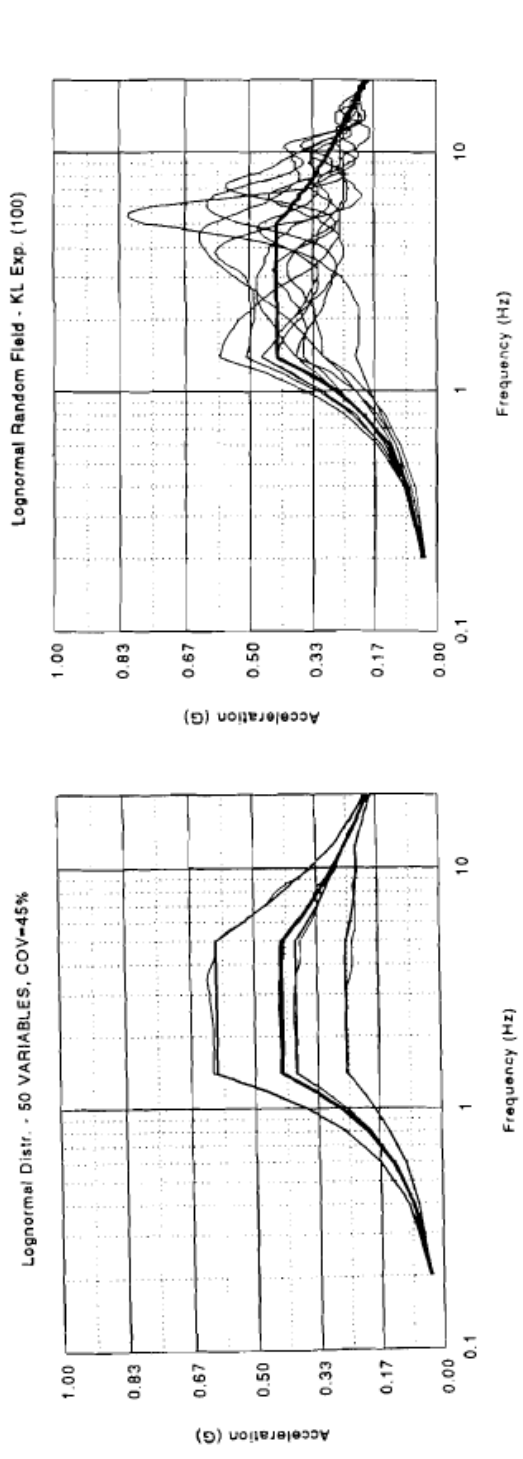


Figure 14. Statistical estimate of probabilistic spectra

Figure 15. Simulated ground spectra

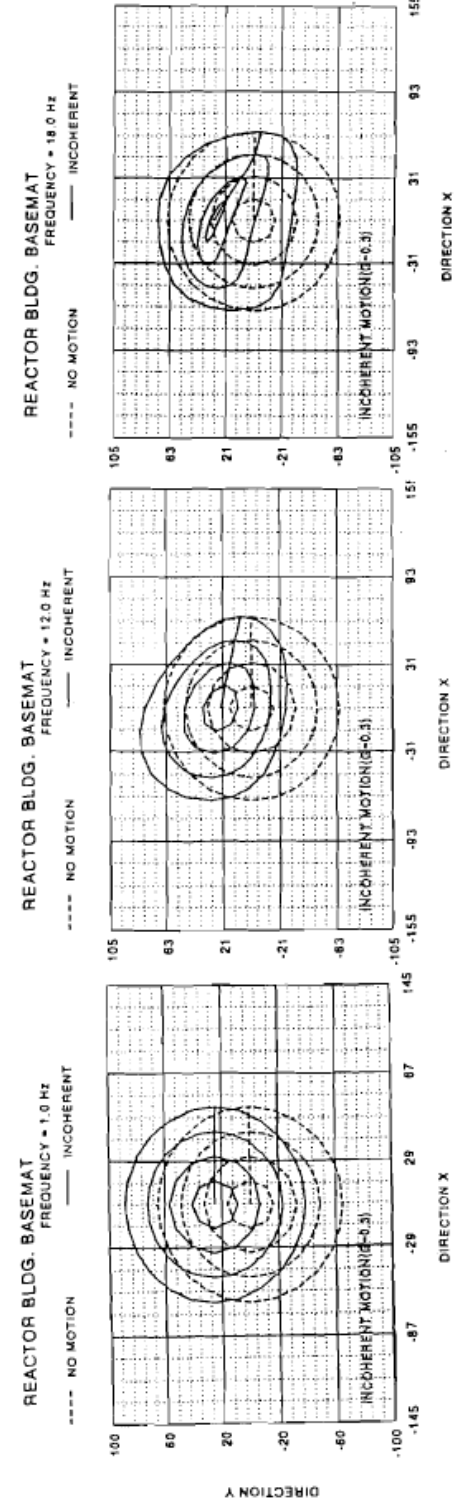
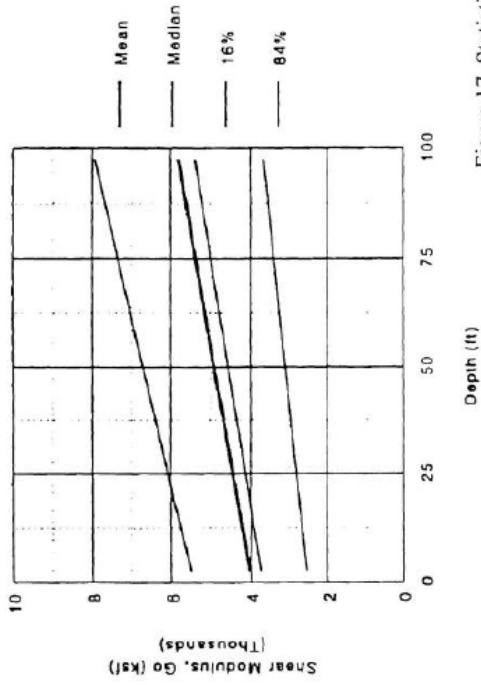


Figure 16. Motion incoherency effects on input

Go Probabilistic Profiles  
Statistical Estimation - Logn. Distr.



Simulated Go Profiles - KL Expansion  
Lognormal Distr. - 20 VARIABLES, COV=40%

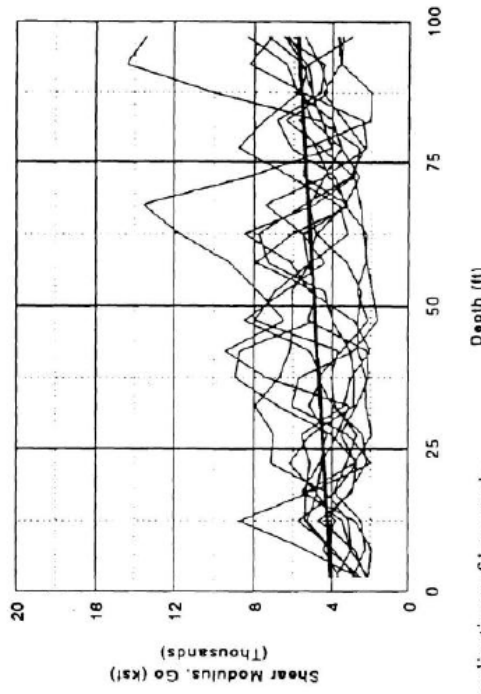


Figure 17. Statistics and realizations of low strain shear modulus profile

Statistical Shear Modulus Curves,  $G_{eff}/G_o$   
Normal Random Field - 11 variables

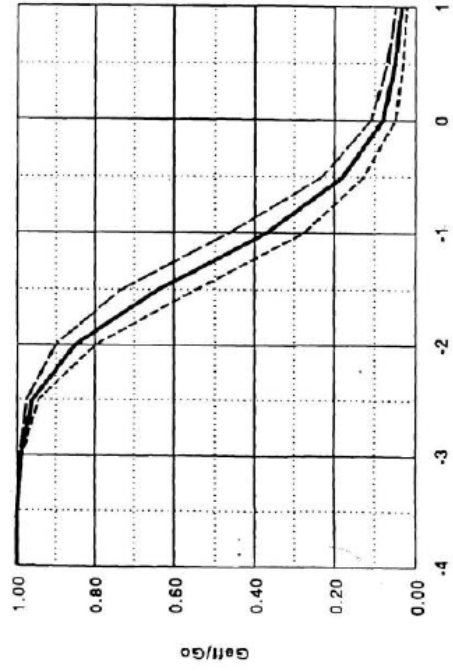
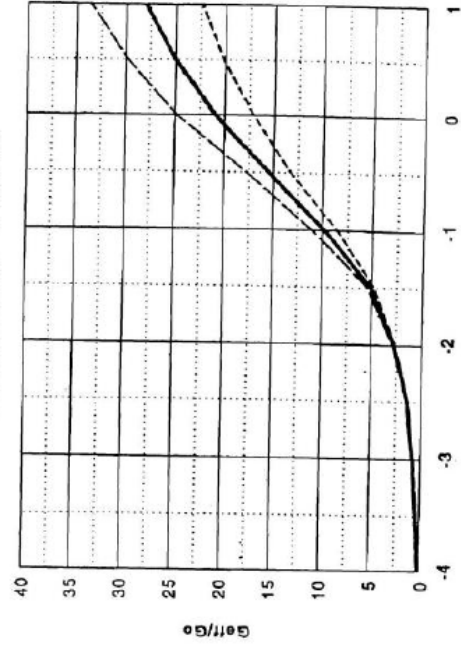
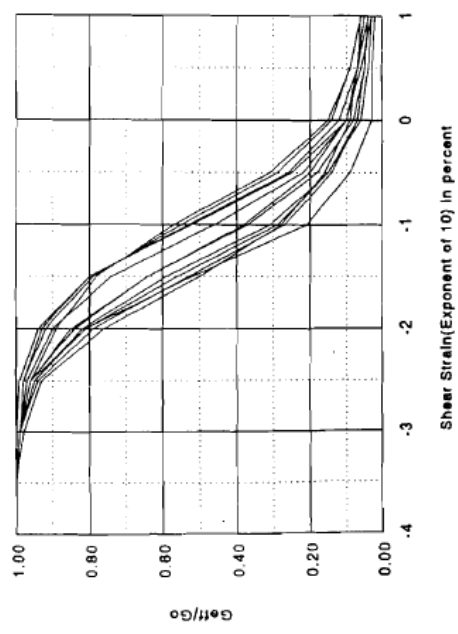


Figure 18. Statistical curves for variations of soil properties with shear strain

Statistical Damping Ratio Curves,  $D_{eff}$   
Normal Random Field - 11 variables



Simulated Shear Modulus Curves,  $G_{eff}/G_0$   
Normal Random Field - 11 variables



Simulated Damping Ratio Curves,  $D_{eff}$   
Normal Random Field - 11 variables

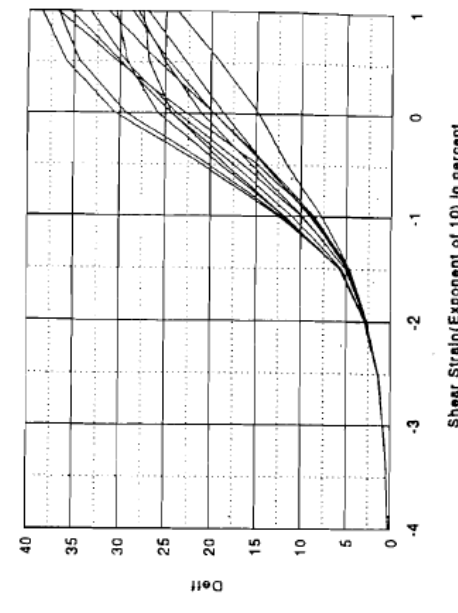


Figure 19. Simulated curves for variations of soil properties with shear strain

TOP OF CONTAINMENT-MCS(500) VS THCE(100)  
ACCELERATION AT 2.00 HZ FREQUENCY

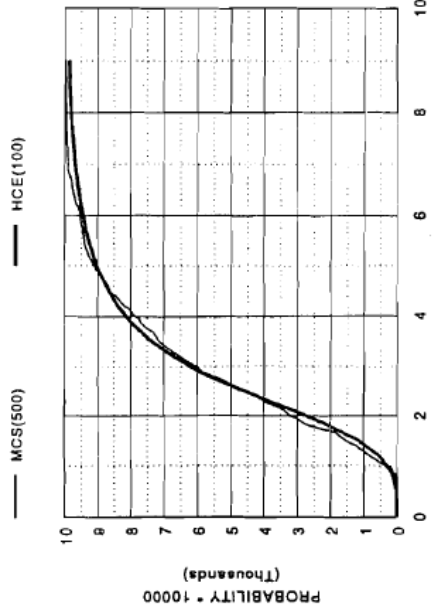


Figure 20. Comparison of probabilistic results

Containment Shell - Base Moment  
Transformed Chaos Expansion Coefficients

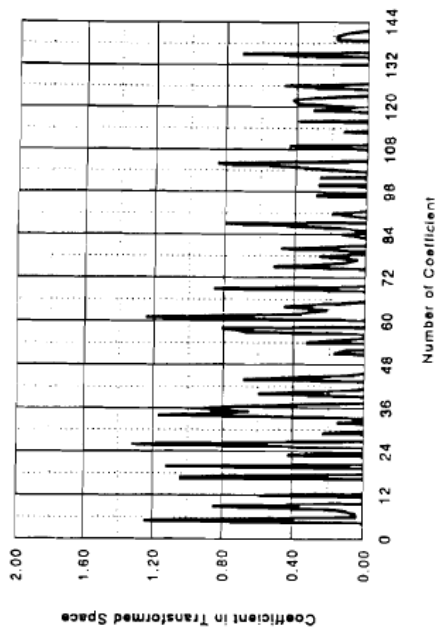
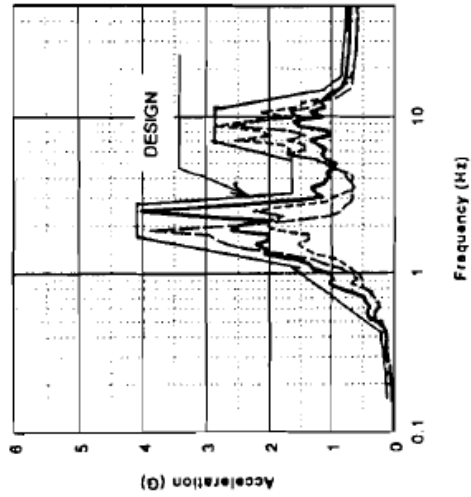
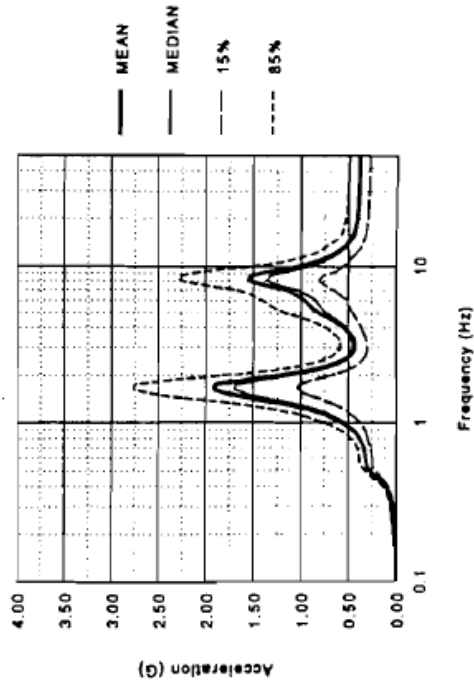


Figure 21. Coefficient of chaos expansion

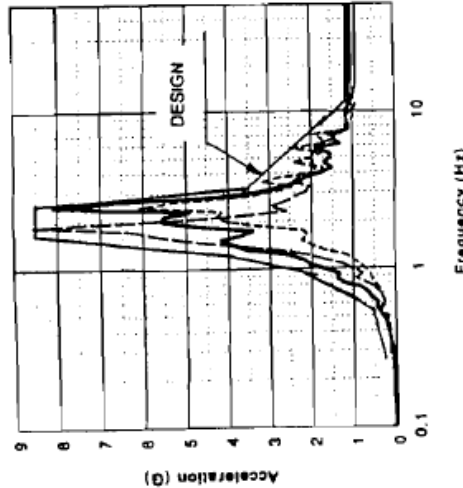
**TOP OF INTERNAL STRUCTURE - Deterministic**  
Variation of Soil Properties, Damping=2%



**Top of Internal Structure Probabilistic**  
Damping=2%



**TOP OF CONTAINMENT SHELL - Deterministic**  
Variation of Soil Properties, Damping=2%



**Top of Containment Shell Probabilistic**  
Damping=2%

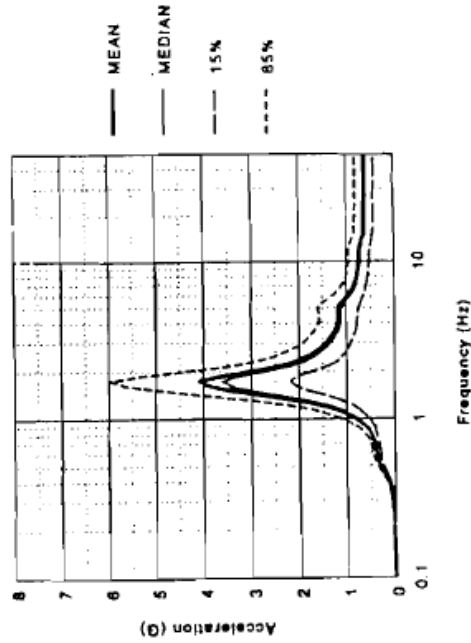


Figure 22. Probabilistic vs. deterministic in-structure response spectra